INORGANIC CHEMISTRY
FRONTIERS

RESEARCH ARTICLE

View Article Online
View Journal

Cite this: DOI: 10.1039/c8qi00652k

A fluorine-functionalized microporous In-MOF with high physicochemical stability for light hydrocarbon storage and separation†

Weidong Fan,‡ Xiuping Liu,‡ Xia Wang, Yue Li, Chengyong Xing, Yutong Wang, Wenyue Guo, Liangliang Zhang and Daofeng Sun *

Received 5th July 2018,
Accepted 13th August 2018

DOI: 10.1039/c8qi00652k

rsc.li/frontiers-inorganic

The storage and separation of hydrocarbons is of great importance for the petrochemical industry. Herein, we report a fluorine-functionalized microporous indium (In) metal–organic framework (UPC-104) for light hydrocarbon storage and separation. UPC-104 can be stable up to 300 °C, and can retain its framework in acidic and alkaline aqueous solutions (pH 1–11). Remarkably, the material exhibits very high H_2 (230.8 $cm^3\ g^{-1}$, 2.06 wt% at 77 K and 1 bar), C_2H_2 (187.0 $cm^3\ g^{-1}$ at 273 K and 1 bar), and C_3H_6/C_3H_8 adsorption capacity (276.5 $cm^3\ g^{-1}$ and 250.4 $cm^3\ g^{-1}$ for C_3H_6 and C_3H_8 at 273 K and 1 bar), and shows potential for the separation of light hydrocarbons (C_2H_2, C_2H_4, C_2H_6, C_3H_6, C_3H_8, n-C_4H_{10}, and i-C_4H_{10} relative to CH_4), as shown by single component gas sorption and selectivity calculations.

The storage and separation of light hydrocarbons is a very important industrial process.[1–3] Hydrocarbons include alkynes, olefins, alkanes, and aromatics, and are important raw materials for the production of various lifestyle and industrial products. Light hydrocarbon gases (CH_4, C_2H_2, C_2H_4, C_2H_6, C_3H_6, C_3H_8, n-C_4H_{10}, and i-C_4H_{10}) are important constituents of hydrocarbons.[4,5] Light hydrocarbon gases play a vital role in the petrochemical industry due to their utilization as fuels or raw materials. For example, methane can replace gasoline and diesel as a clean fuel for automobiles, acetylene and ethylene have been used as raw materials for the production of industrial products such as acetic acid, rubber and plastics, and propylene can be used for the production of acrylonitrile, propylene oxide, and polypropylene.[6–8] Therefore, obtaining high-quality and high-purity light hydrocarbon gas is the key to ensuring its effective use. It is of great significance to study how to efficiently separate light hydrocarbon gases in industrial production. Conventional light hydrocarbon separation usually adopts energy-intensive cryogenic distillation technology.[9] In order to obtain a single product, it often requires multi-step distillation and high reflux ratio. To this end, how to realize the separation of light hydrocarbons with low energy consumption is a technical problem that urgently needs to be solved in actual production.[10]

Adsorption and desorption of gas using a porous material at a specific temperature and pressure is an effective method for separating gas mixtures. Metal–organic frameworks (MOFs) are porous crystalline materials, and structurally and functionally regulated by reasonable choice of functional organic ligands and various metal ions, and thus have potential application value in the field of gas capture and separation.[11–14] However, most MOFs based on low-valence transition metal ions such as Cu^{2+} and Zn^{2+} are prone to hydrolysis and hence suffer from poor chemical stability,[15] thus frequently limiting their practical application. One way to solve this issue is to introduce higher valence metal cations such as M^{3+} (M = In, Al, Fe, Cr) or M^{4+} (Zr, Hf) cations to assemble MOFs for enhancing thermal and chemical stabilities.[16,17] However, this makes it harder to control the formation of MOFs due to the higher reactivity of these higher valence metal cations. One important parameter is the charge density of the cation in solution, which depends on the ionic radius and charge. For instance, high pH has to be reached to produce metal hydroxides for divalent cations, but it is much easier to produce metal oxides or hydroxides for higher valence cations over a larger pH range, which will restrict drastically the conditions to produce crystalline MOFs from these reactive cations.[18–20] There are exceptions to the instability of MOFs prepared with low valent cations. In particular, the MOF-74/CPO-27/M-DOBDC (M = Fe^{2+}, Mg^{2+}) series is reasonably stable and exhibits excellent performance for hydrocarbon separation.[21]

State Key Laboratory of Heavy Oil Processing, College of Science, China University of Petroleum (East China), Qingdao, Shandong, 266580, People's Republic of China. E-mail: dfsun@upc.edu.cn

†Electronic supplementary information (ESI) available: Experimental, characterization and additional figures. CCDC 1837588. For ESI and crystallographic data in CIF or other electronic format see DOI: 10.1039/c8qi00652k

‡These authors contributed equally to this work.

The lower abundance of In limits the use of compounds and materials containing In. However, In-MOF exhibits very low acute toxicity and high thermal and chemical stability. On the other hand, the adsorbent can be reused in gas adsorption and separation applications. Therefore, In-MOF can be considered as an ideal candidate for gas adsorption and separation.[22] In this communication, we report a new In-MOF $\{[In_{1.5}(\mu_3\text{-}O)_{0.5}(TPTA\text{-}F)(H_2O)(OH)_{0.5}]\cdot 4DMF\cdot 4.5H_2O\}$ (denoted as **UPC-104**) based on a fluorine-functionalized tricarboxylate ligand (H_3TPTA-F = 2′-fluoro-[1,1′:3′,1″-terphenyl]-4,4″,5′-tricarboxylic acid) with C_2 symmetry. **UPC-104** consists of two different types of hollow cages with accessible diameters of about 13.0 and 21.8 Å. It is interesting that the material demonstrates high hydrothermal and chemical stability. Significantly, single component gas sorption and selectivity calculations reveal that the porous **UPC-104** exhibits high C_3H_8, C_3H_6, and C_2H_2 adsorption capacity and shows high separation selectivity for C_4H_n, C_3H_n and C_2H_n light hydrocarbons relative to CH_4, indicating that **UPC-104** could be a promising candidate for fuel gas purification and light hydrocarbon storage and separation.

Colorless block crystals of **UPC-104** were obtained by a solvothermal reaction between H_3TPTA-F and $In(NO_3)_3\cdot 4.5H_2O$ in *N*,*N*′-dimethylformamide (DMF) at 100 °C for three days (ESI†). The phase purity of **UPC-104** was confirmed using powder X-ray diffraction (PXRD). Single-crystal X-ray structural analysis reveals that **UPC-104** crystallizes in the trigonal system with the *Rpc* space group, and the asymmetric unit contains one and a half In^{III} ions, one fully deprotonated TPTA-F^{3-} ligand (Fig. 1a), a half bridging μ_3-O^{2-} moiety, one coordinated water molecule, and a half coordinated hydroxyl. Every In^{III} ion is typically six-coordinated by four carboxylate oxygen atoms from four TPTA-F^{3-} ligands, one oxygen atom from bridging μ_3-O^{2-}, and one oxygen atom from a coordinated water molecule or hydroxyl, giving an octahedral coordination configuration (Fig. 1b). Two In1 and one In2 are connected to each other through one μ_3-O^{2-} and six $-COO^-$, to form a classic $[In_3(\mu_3\text{-}O)(COO)_6]$ cluster. Each TPTA-F^{3-} ligand connects to three $[In_3(\mu_3\text{-}O)(COO)_6]$ clusters using its three carboxylate groups, with the average bond length of 2.162 Å. **UPC-104** consists of two different types of hollow cages: the larger cage is formed by 12 metal clusters connected by ligands with an accessible diameter of about 21.8 Å, and the smaller cage is formed by six metal clusters with an accessible diameter of about 13.0 Å (Fig. 1c, and Fig. S1†). From the viewpoint of topology, we can simplify both the $[In_3(\mu_3\text{-}O)(COO)_6]$ cluster as a six-connected node and the TPTA-F^{3-} ligand as a three-connected node. As a result, **UPC-104** adopts a 3,6-c uninodal net with a topological point symbol of $\{4\cdot 6^2\}_2\{4^2\cdot 6^7\cdot 8^6\}$ (Fig. 1d–f).

The solvent accessible volume of **UPC-104** calculated using PLATON is 70.8% (35 075 $Å^3$ out of the 49 486 $Å^3$ unit cell volume), and 7375 electrons were removed from the unit-cell contents.[23] In the *Rpc* space group, the asymmetric unit is 1/36 of the unit cell; so, the asymmetric unit would have contributed 7375/36 = 205 electrons, corresponding to four DMF molecules (4 × 40 electrons) and four and a half H_2O molecules (4.5 × 10 electrons).[24]

Hydrothermal and chemical stability are important for host materials with the potential for industrial application, and can be demonstrated using powder X-ray diffraction (PXRD) (Fig. 2). The PXRD pattern of **UPC-104** heated at different temperatures showed similar diffraction peaks at least up to 300 °C, demonstrating its high thermal stability, which is consistent with the results observed from thermogravimetric analysis (TGA) (Fig. S6†). By soaking the crystals of **UPC-104** in the acid (HCl) or alkali (NaOH) aqueous solution, it was confirmed that the framework of **UPC-104** can be stable in the pH range of 1–11. The excellent thermal and chemical stabilities may be attributed to the synergistic effect of $[In_3(\mu_3\text{-}O)(COO)_6]$ clusters and the strong coordination interactions between In^{III} and carboxylate groups.

The permanent porosity of **UPC-104** was confirmed by its N_2 adsorption isotherm (Fig. 3a). After desolvation, **UPC-104** exhibits a N_2 gas uptake of 749.49 $cm^3\ g^{-1}$, revealing a Brunauer–Emmett–Teller (BET) surface area of 2592.54 $m^2\ g^{-1}$ (Langmuir 2912.65 $m^2\ g^{-1}$), a pore volume of 0.121 $cm^3\ g^{-1}$, and a primary pore size distribution of ~11.2 Å (Fig. 3b), which are slightly less than the crystallographic data deter-

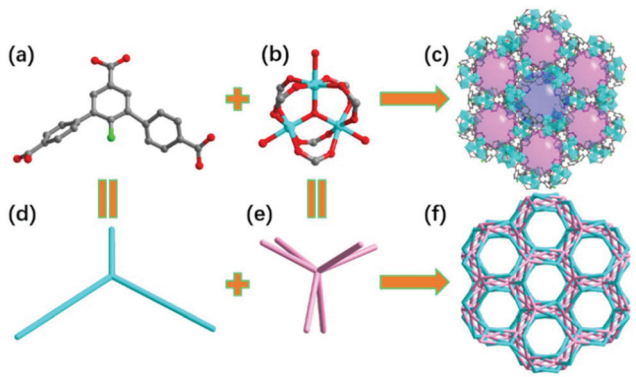

Fig. 1 (a and b) Ligand used in this work, and the trinuclear metal clusters in **UPC-104**. (c) Two types of hollow cages in **UPC-104**. (d, e, and f) Topological analysis of **UPC-104**.

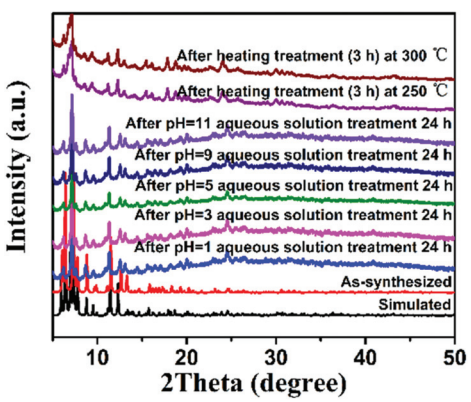

Fig. 2 Powder X-ray diffraction (PXRD) of **UPC-104**.

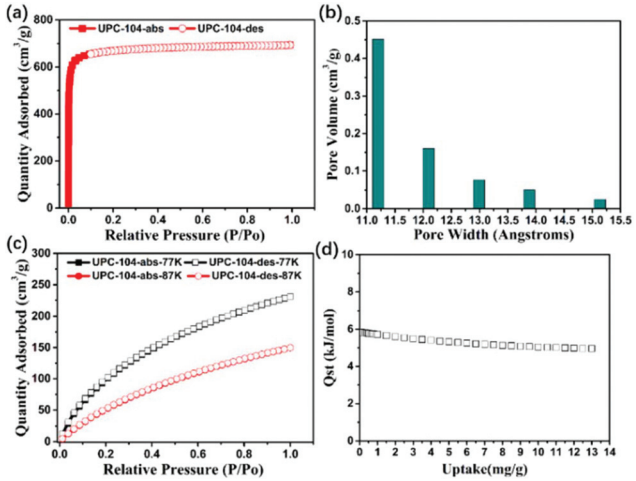

Fig. 3 (a and b) N_2 sorption isotherm (77 K) and pore-size distribution for **UPC-104**. (c and d) H_2 sorption isotherm (77 K and 87 K) and adsorption heat (Q_{st}) for **UPC-104**.

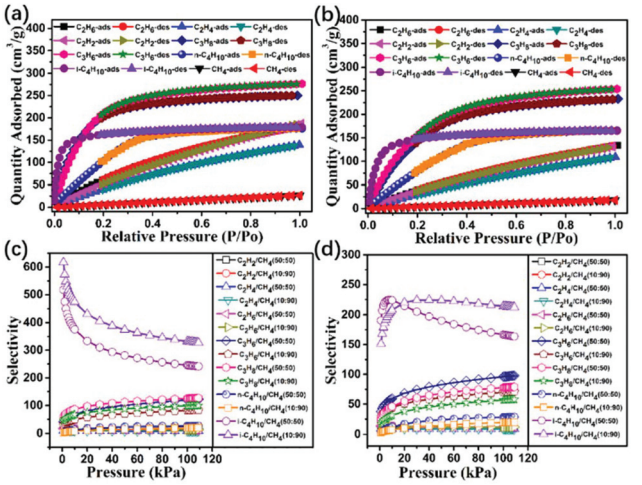

Fig. 4 The CH_4, C_2H_6, C_2H_4, C_2H_2, C_3H_8, C_3H_6, n-C_4H_{10}, and i-C_4H_{10} adsorption isotherms at 273 K (a) and 298 k (b), respectively, for **UPC-104**; the selectivity for C_2H_6, C_2H_4, C_2H_2, C_3H_8, C_3H_6, n-C_4H_{10}, and i-C_4H_{10} over CH_4 at 273 K (c) and 298 k (d), respectively, for **UPC-104**.

mined using single crystal X-ray diffraction. The H_2 uptake capacity of **UPC-104** at 77 K (Fig. 3c) is up to 230.8 $cm^3\ g^{-1}$ (2.06 wt%), which is comparable to those of well-known microporous MOF materials (Table S5†). The H_2 adsorption isotherms at 77 K and 87 K were collected, and the adsorption enthalpy (Q_{st}) was calculated using the Clausius–Clapeyron equation. The value at the zero coverage for **UPC-104** is calculated to be 5.84 kJ mol^{-1} (Fig. 3d), which is higher than that of MOF-5 (5.2 kJ mol^{-1}),[25] and is comparable to that of NOTT-122 (6.0 kJ mol^{-1}).[26]

Due to its unique pore structure with open metal sites and high physicochemical stability, **UPC-104** possesses potential application for light hydrocarbon adsorption and separation. Thus, low-pressure C_3H_6 and C_3H_8 uptakes were further measured under 1 bar. As expected, the C_3H_6 and C_3H_8 adsorption amounts for **UPC-104** reach up to 276.5 $cm^3\ g^{-1}$ and 250.4 $cm^3\ g^{-1}$ at 273 K and 1 bar, respectively, which is a record in the reported MOF materials for C_3H_6 and C_3H_8 uptake (Fig. 4a). In practice, C_3H_6 and C_3H_8 gases are normally stored at ambient temperature. Therefore, the C_3H_6 and C_3H_8 adsorption experiments were carried out at room temperature (298 K). Exhilaratingly, **UPC-104** exhibits adsorption amounts of 253.9 and 232.8 $cm^3\ g^{-1}$ for C_3H_6 and C_3H_8 (Fig. 4b), respectively, which is dramatically higher than those of UPC-21 (116.2 and 124.1 $cm^3\ g^{-1}$), UPC-33 (94.3 and 93.6 $cm^3\ g^{-1}$),[24] FJI-C1 (160.9 $cm^3\ g^{-1}$ for C_3H_8) and FJI-C4 (74.7 $cm^3\ g^{-1}$ for C_3H_8).[10] In addition, **UPC-104** exhibits higher C_2H_2, C_2H_4, C_2H_6, n-C_4H_{10}, and i-C_4H_{10} adsorptions of 187.0, 139.1, 180.6, 176.1, and 178.8 $cm^3\ g^{-1}$ at 273 K and 1 bar, respectively (Fig. 4a). The acetylene uptake capacity of **UPC-104** is comparable to those of the reported MOFs (Table S6†), such as MgMOF-74 (184 $cm^3\ g^{-1}$),[27] NOTT-101 (184 $cm^3\ g^{-1}$),[28] and ZJU-10a (174 $cm^3\ g^{-1}$),[29] and even higher than those of some well-known MOFs, UTSA-20 (150 $cm^3\ g^{-1}$),[28] MOF-505 (148 $cm^3\ g^{-1}$),[30] and UMCM-150 (129 $cm^3\ g^{-1}$).[28] Even when the temperature was raised to 298 K, the C_2H_2, C_2H_4, C_2H_6, n-C_4H_{10}, and i-C_4H_{10} adsorption amounts could also reach up to 131.0, 108.7, 133.8, 165.1, and 164.8 $cm^3\ g^{-1}$ (Fig. 4b). Clearly, **UPC-104** might be a good candidate for C_4H_n, C_3H_n and C_2H_n storage under ambient conditions.

Compared with C_4H_n, C_3H_n and C_2H_n adsorption, the amount of CH_4 (26.6 $cm^3\ g^{-1}$ for 273 K, and 18.1 $cm^3\ g^{-1}$ for 298 K, at 1 bar) adsorbed by **UPC-104** is very low, which should be related to the weak guest–host interactions between gas molecules and the MOF framework. The magnitude of the adsorption enthalpies reveals the affinity of the pore surface toward adsorbents, which plays a significant part in determining the adsorptive selectivity. To evaluate the affinity of such light hydrocarbons in **UPC-104**, the enthalpies of adsorption were calculated by the Clausius–Clapeyron equation. The adsorption enthalpies of CH_4, C_2H_2, C_2H_4, C_2H_6, C_3H_6, C_3H_8, n-C_4H_{10}, and i-C_4H_{10} were 8.8, 10.3, 10.4, 15.1, 14.6, 26.5, 19.7, and 41.7 kJ mol^{-1} at zero coverage, respectively (Fig. 4d).

The light hydrocarbons with higher adsorption enthalpies [Q_{st}(i-C_4H_{10}) > Q_{st}(C_3H_8) > Q_{st}(n-C_4H_{10}) > Q_{st}(C_2H_6) > Q_{st}(C_3H_6) > Q_{st}(C_2H_4) > Q_{st}(C_2H_2) > Q_{st}(CH_4)] may provide stronger affinity with a skeleton, which results in these gases being preferentially adsorbed onto the skeleton of **UPC-104**. Thus, it may have high selectivity of C_4H_n, C_3H_n and C_2H_n light hydrocarbons relative to CH_4. Therefore, the potential for the separation of CH_4 from C_4H_n, C_3H_n and C_2H_n light hydrocarbons was appraised by the ideal solution adsorbed theory (IAST) for binary equimolar components (Fig. S7†). At 1 bar and 273 K, the selectivities of i-C_4H_{10}, C_3H_8, and C_3H_6 to CH_4 are 241.5, 126.9, and 122.5, which are higher than n-C_4H_{10}, C_2H_6, C_2H_4, and C_2H_2 to CH_4 for 26.1, 14.3, 8.5 and 12.0, respectively (Fig. 4c). At 1 bar and 298 K, the selectivities of i-C_4H_{10}, C_3H_8, and C_3H_6 to CH_4 are 163.7, 79.0, and 97.9, which are also

higher than *n*-C_4H_{10}, C_2H_6, C_2H_4, and C_2H_2 to CH_4 for 28.5, 12.3, 8.9 and 11.8, respectively (Fig. 4d). It should be noted that these values compare with those for gea-MOF-1 (200, C_4H_{10}/CH_4 = 5/95),[31] UPC-21 (75 for C_3H_6/CH_4, 67 for C_3H_8/CH_4), and FJI-C1 (78.7 for C_3H_8/CH_4).[10] The results indicate that **UPC-104** is a prospective adsorbent for the separation of C_4H_n and C_3H_n hydrocarbons from CH_4 at 298 K. The high adsorption selectivity of C_4H_n–C_3H_n/CH_4 could be attributed to the special pore shape and internal surface functionality (fluoro–) of pores in the MOFs.

To better understand the adsorption performance of **UPC-104** at the molecular level, we have performed the GCMC simulations using the Sorption code.[32] To probe the distribution features of the C_3H_6 molecules in **UPC-104**, we further analyzed the density distribution of the center mass of C_3H_6 molecules from GCMC simulations. As shown in Fig. 5, the results from GCMC simulations at 298 K and 5 kPa indicate that C_3H_6 molecules in **UPC-104** mainly adhere to the cages, which may have strong overlapping potentials. As for the whole structure, the C_3H_6 molecules prefer to locate in the open In^{III} sites, fluorine groups and the electron-dense aromatic rings within the framework.

To further probe the advantages of the open In^{III} sites and fluorine groups for gas adsorption, DFT calculations were performed on **UPC-104**. The optimized structures and the corresponding adsorption energies are presented in Fig. S33.† The adsorption energies of the C_2H_2 and C_3H_6 molecules at the open In^{III} site in **UPC-104** are −30.93 and −48.53 kJ mol^{-1}, and for that at the fluorine site in **UPC-104** are −28.39, and −39.14 kJ mol^{-1}. The distance between the H atom of C_2H_2/C_3H_6 and the fluorine group is 2.3 and 2.56 Å, which is smaller than the sum of the van der Waals radius of the H and F atoms (2.61 Å), indicating the existence of a strong F···H–C hydrogen bond.[33] The phenomenon might be due to the enhancement of the polarization on the C_3H_6 molecule induced by the functional groups *via* the electrical field-quadrupole interactions.

In summary, an ultra-stable microporous In-MOF **UPC-104** based on a fluorine-functionalized tricarboxylate ligand has been synthesized and structurally characterized. In the presented structure, the $[In_3(\mu_3\text{-}O)(COO)_6]$ clusters are linked by the tricarboxylate ligands to form a highly porous framework with two different types of hollow cages. Single component gas sorption and selectivity calculations reveal that **UPC-104** exhibits very high hydrogen, acetylene and propene/propane adsorption capacity and shows potential for the separation of C_4H_n, C_3H_n and C_2H_n light hydrocarbons from CH_4, indicating that **UPC-104** could be a promising candidate for fuel gas purification and separation of light hydrocarbons. GCMC and first-principle calculations indicate that the functional fluorine groups and open metal sites could enhance the gas–framework interactions. Benefitting from the straightforward design of MOFs with modifiable performance, development of customizable and stable adsorbents for energy gas storage and separation, such as C_2H_2/C_2H_4, C_3H_6/C_3H_8, *etc.*, is currently underway.

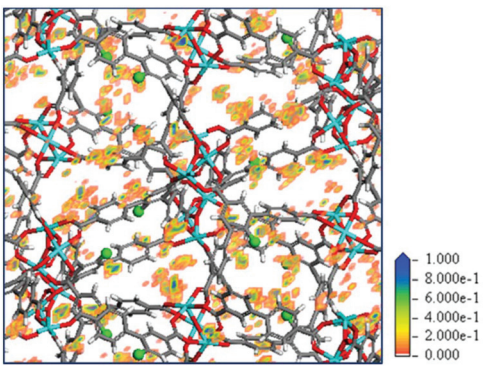

Fig. 5 Density distribution of the center of C_3H_6 in **UPC-104** obtained from GCMC simulations at 5 kPa and 298 K.

Conflicts of interest

There are no conflicts to declare.

Acknowledgements

We are grateful for financial support from the National Natural Science Foundation of China (NSFC, Grant No. 21571187), the Taishan Scholar Foundation (ts201511019) and the Fundamental Research Funds for the Central Universities (18CX06003A).

Notes and references

1 P. Silva, S. M. F. Vilela, J. P. C. Tomé and F. A. Almeida Paz, *Chem. Soc. Rev.*, 2015, **44**, 6774–6803.
2 M. Du, C.-P. Li, M. Chen, Z.-W. Ge, X. Wang, L. Wang and C.-S. Liu, *J. Am. Chem. Soc.*, 2014, **136**, 10906–10909.
3 R. A. Agarwal and N. K. Gupta, *Coord. Chem. Rev.*, 2017, **332**, 100–121.
4 K. Adil, Y. Belmabkhout, R. S. Pillai, A. Cadiau, P. M. Bhatt, A. H. Assen, G. Maurin and M. Eddaoudi, *Chem. Soc. Rev.*, 2017, **46**, 3402–3430.
5 Y. B. He, B. Li, M. O'Keeffe and B. L. Chen, *Chem. Soc. Rev.*, 2014, **43**, 5618–5656.
6 Z.-J. Guo, J. M. Yu, Y.-Z. Zhang, J. Zhang, Y. Chen, Y. F. Wu, L.-H. Xie and J.-R. Li, *Inorg. Chem.*, 2017, **56**, 2188–2197.
7 Y.-X. Tan, Y. A. Si, W. J. Wang and D. Q. Yuan, *J. Mater. Chem. A*, 2017, **5**, 23276–23282.
8 J.-W. Zhang, M.-C. Hu, S.-N. Li, Y.-C. Jiang, P. Qu and Q.-G. Zhai, *Chem. Commun.*, 2018, **54**, 2012–2015.
9 R.-B. Lin, L. B. Li, H. Wu, H. Arman, B. Li, R.-G. Lin, W. Zhou and B. L. Chen, *J. Am. Chem. Soc.*, 2017, **139**, 8022–8028.
10 L. Li, X. S. Wang, J. Liang, Y. B. Huang, H. F. Li, Z. J. Lin and R. Cao, *ACS Appl. Mater. Interfaces*, 2016, **8**, 9777–9781.

11 D. Tian, J. Xu, Z.-J. Xie, Z.-Q. Yao, D.-L. Fu, Z. Zhou and X.-H. Bu, *Adv. Sci.*, 2015, 1500283.
12 F.-M. Zhang, L.-Z. Dong, J.-S. Qin, W. Guan, J. Liu, S.-L. Li, M. Lu, Y.-Q. Lan, Z.-M. Su and H.-C. Zhou, *J. Am. Chem. Soc.*, 2017, **139**, 6183–6189.
13 B. Li, X. L. Cui, D. O'Nolan, H.-M. Wen, M. D. Jiang, R. Krishna, H. Wu, R.-B. Lin, Y.-S. Chen, D. Q. Yuan, H. X. Xing, W. Zhou, Q. L. Ren, G. D. Qian, M. J. Zaworotko and B. L. Chen, *Adv. Mater.*, 2017, 1704210.
14 S. Yuan, L. Feng, K. C. Wang, J. D. Pang, M. Bosch, C. Lollar, Y. J. Sun, J. S. Qin, X. Y. Yang, P. Zhang, Q. Wang, L. F. Zou, Y. M. Zhang, L. L. Zhang, Y. Fang, J. L. Li and H.-C. Zhou, *Adv. Mater.*, 2018, 1704303.
15 W. D. Fan, H. Lin, X. Yuan, F. N. Dai, Z. Y. Xiao, L. L. Zhang, L. W. Luo and R. M. Wang, *Inorg. Chem.*, 2016, **55**, 6420–6425.
16 Q.-G. Zhai, X. H. Bu, C. Y. Mao, X. Zhao and P. Y. Feng, *J. Am. Chem. Soc.*, 2016, **138**, 2524–2527.
17 Q.-G. Zhai, X. H. Bu, X. Zhao, D.-S. Li and P. Y. Feng, *Acc. Chem. Res.*, 2017, **50**, 407–417.
18 Y. Bai, Y. B. Dou, L. H. Xie, W. Rutledge, J.-R. Li and H.-C. Zhou, *Chem. Soc. Rev.*, 2016, **45**, 2327–2367.
19 J.-H. Wang, Y. Zhang, M. Li, S. Yan, D. Li and X.-M. Zhang, *Angew. Chem., Int. Ed.*, 2017, **56**, 6478–6482.
20 C. Serre, F. Millange, C. Touvenot, M. Nogues, G. Marsolier, D. Louër and G. Férey, *J. Am. Chem. Soc.*, 2002, **124**, 13519–13526.
21 E. D. Bloch, W. L. Queen, R. Krishna, J. M. Zadrozny, C. M. Brown and J. R. Long, *Science*, 2012, **335**, 1606–1610.
22 X. J. Li, X. Y. Chen, F. L. Jiang, L. Chen, S. Lu, Q. H. Chen, M. Y. Wu, D. Q. Yuan and M. C. Hong, *Chem. Commun.*, 2016, **52**, 2277–2280.
23 A. L. Spek, *PLATON, A multipurpose crystallographic tool*, Utrecht University, The Netherlands, 2001.
24 W. D. Fan, Y. T. Wang, Q. Zhang, A. Kirchon, Z. Y. Xiao, L. L. Zhang, F. N. Dai, R. M. Wang and D. F. Sun, *Chem. – Eur. J.*, 2018, **24**, 2137–2143.
25 S. Q. Ma, J. M. Simmons, D. Q. Yuan, J.-R. Li, W. Weng, D.-J. Liu and H.-C. Zhou, *Chem. Commun.*, 2009, 4049–4051.
26 Y. Yan, M. Suyetin, E. Bichoutskaia, A. J. Blake, D. R. Allan, S. A. Barnett and M. Schröder, *Chem. Sci.*, 2013, **4**, 1731–1736.
27 S. C. Xiang, W. Zhou, Z. J. Zhang, M. A. Green, Y. Liu and B. L. Chen, *Angew. Chem., Int. Ed.*, 2010, **49**, 4615–4618.
28 Y. B. He, R. Krishna and B. L. Chen, *Energy Environ. Sci.*, 2012, **5**, 9107–9120.
29 X. Duan, H. Z. Wang, Z. G. Ji, Y. J. Cui, Y. Yang and G. D. Qian, *J. Solid State Chem.*, 2016, **241**, 152–156.
30 S. C. Xiang, W. Zhou, J. M. Gallegos, Y. Liu and B. L. Chen, *J. Am. Chem. Soc.*, 2009, **131**, 12415–12419.
31 V. Guillerm, Ł. J. Weseliński, Y. Belmabkhout, A. J. Cairns, V. D'Elia, Ł. Wojtas, K. Adil and M. Eddaoudi, *Nat. Chem.*, 2014, **6**, 673–680.
32 X. Li, Y. Jin, Q. Xue, L. Zhu, W. Xing, H. Zheng and Z. Liu, *J. CO_2 Util.*, 2017, **18**, 275–282.
33 G. R. Desiraju and T. Steiner, *The weak hydrogen bond: in structural chemistry and biology*, Oxford University Press, 2001.